2019 IEEE/RSJ International Conference on Intelligent Robots and Systems (IROS)
Macau, China, November 4-8, 2019

On the Feasibility of Multi-Degree-of-Freedom Haptic Devices Using Passive Actuators

Maciej Łącki, and Carlos Rossa

Abstract— **Stability and transparency are key design requirements in haptic devices. Transparency can be significantly improved by replacing conventional electric motors with passive actuators such as brakes or dampers. Passive actuators can display a wide range of impedance and since they can only dissipate energy, stability is guaranteed. However, passive haptic devices suffer from a serious drawback; the direction of the force output is difficult to control. This issue was addressed extensively for planar manipulators but devices with higher degrees-of-freedom (DOF) have not been examined.**

In this paper, we introduce a new analytical framework to evaluate the feasibility and performance of non-redundant passive haptic manipulators with any DOF. The method identifies different regions in the workspace where a force can be created or approximated, and regions where a passive system cannot create force at all for a given user input. The results indicate that the range of forces a passive device can display increases with the number of DOF. This framework can aid in the design of control methods for multi-DOF passive haptic devices.

I. Introduction

The ideal haptic device is mechanically invisible to the user; it has no friction and no inertia, it can display an infinite range of impedance while maintaining stability. Traditionally, haptic devices employ electric motors to generate force feedback. These devices suffer from stability issues and thus they need to dissipate energy to maintain stability. This poses an inherent trade-off between stability and the fidelity of the haptic rendering [1]–[3].

One way of improving the performance of a haptic device is to replace motors with passive actuators such as electric brakes [4]. Brakes do not suffer from stability issues as they can only dissipate energy. As a result, a passive haptic display can exhibit a larger impedance range than an equivalent active system without becoming unstable [5]–[7]. Passively-actuated haptic devices are therefore a promising alternative in applications requiring high feedback forces such as in surgical simulators [8]–[10], teleoperation [11]–[13], rehabilitation devices [14], [15], and collaborative robots [16], [17].

Book *et al.* [16], [17] were amongst the first to use brakes to produce forces to the user. Their device, P-TER, was a 5 bar redundantly actuated the planar device, designed to assist the user with a trajectory following task. Since then, many other passive haptic devices have been developed, ranging from a 1 degree-of-freedom (DOF) [14], [15], to 2-DOF [8], [11], [13], 3-DOF [9], and 4-DOF [12] systems.

To build these devices some major challenges had to be addressed. For instance, since brakes can only dissipate energy, passive haptic devices cannot generate forces in arbitrary directions. Additionally, the inherent stiction in brakes affects the torque a stationary and moving brake create, resulting in un-smooth force output. These issues have been studied in a 2-DOF device by Cho *et al.* [18]–[20]. They described the regions of the workspace where forces could be generated and the regions where only an approximation of the force could be displayed. To mitigate these issues clever control algorithms had to be developed. An early controller for a passive device was developed to assist a user in following a pre-defined trajectory. The controller approximated a desired force by switching between one actuator at a time [21]. A similar controller was developed in [13]. It also used only one brake at a time to generate a smooth force output while attempting to minimize position error. Cho *et al.* developed a controller in [20] that not only produced smooth force output of a 2-DOF device but also increased the force range. This controller was later improved in [22] by making it less reliant on a force sensor.

Most of the applications and control methods listed above are limited to planar [16]–[22] or 3-DOF manipulators [9]. The question then arises: Are multi-DOF, non-redundant passive manipulators feasible? How will the number of DOF affect the performance of a passive haptic device? In this paper, we propose a new framework to address this question. To the best of our knowledge, a general formulation for an n-DOF passive haptic device has not been presented before. To this end, in Section II we model a 2-DOF device, establish the relationship between force, torque, and velocity, and define regions in the workspace where a desired force can be displayed accurately or partially. Then, in Section III we expand the analysis to develop a general formulation for the force output of an n-DOF device. To illustrate the concept, a 3-DOF device will be examined in Section IV and the concept of *Degree-of-Displayability* is then introduced as a means of quantifying performance. Finally, in Section V we address the constraints bounding the feasibility of an n-DOF device. The proposed framework can be used to aid the design and control of both passive and hybrid multi-DOF haptic devices.

II. Force Modelling of Passive Haptic Devices

Let us begin our analysis by examining the behaviour of a 2-DOF, non-redundant, passive manipulator.

M. Lacki and C. Rossa are with the Faculty of Engineering and Applied Science, Ontario Tech University, Oshawa, ON, Canada. E-mail: maciej.lacki@uoit.ca; carlos.rossa@uoit.ca.

We acknowledge the support of the Natural Sciences and Engineering Research Council of Canada (NSERC), [funding number 2018-06074]. Cette recherche a été financée par le Conseil de recherches en sciences naturelles et en génie du Canada (CRSNG), [numéro de référence 2018-06074].

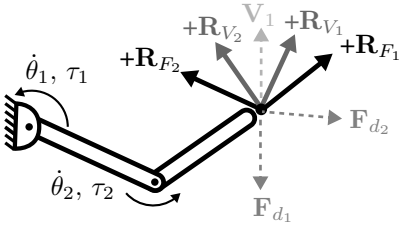

Fig. 1. The reference vectors, desired force, and velocities acting on a 2-DOF manipulator, where each joint is actuated.

A. Passivity Constraint

The force produced by a brake is a result of energy dissipation. For instance, applying a brake in a moving vehicle results in a force acting opposite to the car's direction of motion. If a force is applied to a stationary vehicle the brake will produce a force equal and opposite to the applied force. A haptic device using brakes behaves in much the same way. Typically, the brakes used in haptic devices are rotary; instead of linear velocity they experience an angular velocity $\dot{\theta}$, and instead of force they produce a torque τ_{out}. When a brake is moving ($\dot{\theta} \neq 0$), the torque it produces is:

$$\tau_{out} = \begin{cases} -\operatorname{sgn}(\dot{\theta})|\tau_a| & \text{if } \operatorname{sgn}(\dot{\theta}) \neq \operatorname{sgn}(\tau_d) \\ 0 & \text{otherwise} \end{cases} \tag{1}$$

In other words, a brake can only generate a desired torque τ_d if its direction opposes that of its angular velocity, i.e. $\tau_d\ \dot{\theta} < 0$ [23]. When the brake is stationary ($\dot{\theta} = 0$) the output torque opposes the torque input τ_{in}, thus,

$$\tau_{out} = \begin{cases} -\operatorname{sgn}(\tau_{in})|\tau_d| & \text{if } \operatorname{sgn}(\tau_{in}) \neq \operatorname{sgn}(\tau_d) \\ 0 & \text{otherwise} \end{cases} \tag{2}$$

Throughout this paper, we will refer to (1) and (2) together as the *Passivity Constraint*. To create a force at the end-effector an actuator must satisfy this constraint.

Now, consider the 2-DOF manipulator shown in Fig. 1, which has one brake at each joint. The end-effector of the device is moving with a velocity $\mathbf{V}_1$ while attempting to generate either a force $\mathbf{F}_{d_1}$ or $\mathbf{F}_{d_2}$. In order to apply the passivity constraint to the device, one must first relate the torque and angular velocity at each joint to the force and velocity at the end effector.

B. Manipulator Kinematics

Let $\mathbf{T} \in \mathbb{R}^{j\times 1}$ represent a transformation matrix relating the angular position of each joint to the position and orientation $\mathbf{P} \in \mathbb{R}^{j\times 1} = \mathbf{T}(\boldsymbol{\theta})$ of the end effector where $\boldsymbol{\theta} = [\theta_1\ \theta_2\ \cdots\ \theta_i]^T$ and for a non-redundant, non-under-actuated device $j = 1, 2, \cdots, i$. This convention will be used through the paper. Similarly, let $\mathbf{J} \in \mathbb{R}^{j\times i}$ represent a Jacobian matrix relating angular velocity to the linear velocity $\mathbf{V} \in \mathbb{R}^{j\times 1} = \mathbf{J}\,\dot{\boldsymbol{\theta}}$ of the end effector, where $J_{nm} = \frac{\partial \mathbf{T}_m}{\partial \theta_n}$, and $\dot{\boldsymbol{\theta}} = \frac{d\boldsymbol{\theta}}{dt}$ with $1 \leq m, n \leq j$. Since we will only consider non-redundant manipulators ($i = j$) the Jacobian is a square matrix. The inverse transpose of the Jacobian matrix relates the torque of all joints to the force at the end effector:

$$\mathbf{F} = \left(\mathbf{J}^{-1}\right)^T \boldsymbol{\tau} \tag{3}$$

where $\mathbf{F} \in \mathbb{R}^{j\times 1}$ [24]. Using these relationships we can apply the passivity constraint to each joint thereby identifying regions in the workspace where the passivity constraint is satisfied, that is, the torque and velocity at a given joint have opposite directions. The boundaries or these regions can be found using the reference vectors described below.

C. Reference Vectors

Going back to Fig. 1, the vectors $+\mathbf{R}_{V_1}$ and $+\mathbf{R}_{V_2}$ are the velocities resulting from positive (counter-clockwise) motion of either joint 1 or 2 whereas the other joint is not moving, i.e., $+\mathbf{R}_{V_1} = \mathbf{J}[1\ 0]^T$ (with $\dot{\theta}_1 = 1$ and $\dot{\theta}_2 = 0$), and $+\mathbf{R}_{V_2} = \mathbf{J}[0\ 1]^T$. Let us call vectors obtained using this operation *Reference Velocity Vectors*. Note that this operation simply extracted the n^{th} column from the Jacobian Matrix. Therefore, the reference velocity vectors are the column space of the Jacobian Matrix:

$$\mathbf{J} = \begin{bmatrix} J_{x_1} & J_{x_2} & \cdots & J_{x_i} \\ J_{y_1} & J_{y_2} & & J_{y_i} \\ \vdots & & \ddots & \vdots \\ \underbrace{J_{\gamma_1}}_{\mathbf{R}_{V_1}} & \underbrace{J_{\gamma_2}}_{\mathbf{R}_{V_2}} & \cdots & \underbrace{J_{\gamma_i}}_{\mathbf{R}_{V_n}} \end{bmatrix}_{j\times i} \tag{4}$$

Applying the same procedure to torques and forces gives $+\mathbf{R}_{F_1} = (\mathbf{J}^{-1})^T[1\ 0]^T$ with $\tau_1 = 1$ and $\tau_2 = 0$ and $+\mathbf{R}_{F_2} = (\mathbf{J}^{-1})^T[0\ 1]^T$. Let us call these vectors the *Reference Force Vectors* (see Fig. 1). Together, they determine the sign of angular velocity and torque resulting from the velocity and force at the end-effector as shown in Fig. 2. For example, from Fig. 2a, it is clear that so long as $\mathbf{V}_1$ is within $+\mathbf{R}_{V_1}$ and $+\mathbf{R}_{V_2}$, the joint angular velocities are $\dot{\theta}_1 > 0$ and $\dot{\theta}_2 > 0$. Similarly, from Fig. 2b, we observe the torques required to create $\mathbf{F}_{d_1}$ are $\tau_1 < 0$ and $\tau_2 < 0$. Likewise, $\mathbf{F}_{d_2}$ requires $\tau_1 > 0$ and $\tau_2 < 0$.

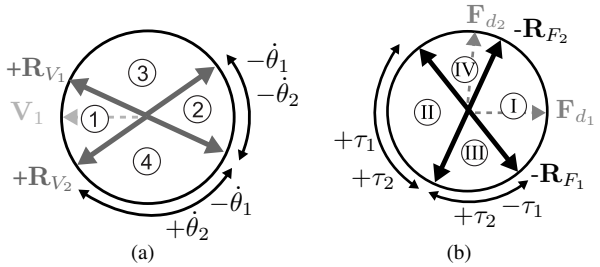

Fig. 2. Intersecting the velocity vectors in (a) and force vectors in (b) produces region pairs. Regions with common numbers are displayable.

D. Displayability Regions

As described before, if the force $\mathbf{F}$ and velocity $\mathbf{V}$ have directions comprised between two of the reference vectors, the direction of torques and angular velocity they create do not change. As a result, the workspace may be divided into 4 distinct regions. In Fig. 2, these regions are labelled with

numbers from I to IV for force, and 1 to 4 for velocity. Force and velocity regions can now be paired according to the passivity constraint.

1) Fully Displayable Region: In Fig. 2a, the input velocity is in region (1), and the forces the device can display are within region (I) in Fig. 2b. This is because the passivity constraint is satisfied for all actuators. Let us refer to region (1) as the *fully-displayable region*. Notice that the size of the fully-displayable region is always a fraction of the total workspace.

2) Partially Displayable Regions: Consider again the end-effector moves with a velocity $\mathbf{V}_1$ and the desired force is $\mathbf{F}_{d_2}$. In this case $\theta_1\tau_1 > 0$ and $\theta_2\tau_2 < 0$ and the passivity constraint is only satisfied in one of the joints. In this region, it is necessary to approximate $\mathbf{F}_{d_2}$ using the actuator that satisfies the constraint. Let us name regions where at least one actuator can be used to approximate the desired force as a *partially displayable region* whose boundaries do not correspond to those from Fig. 2b and will now be defined.

Fig. 3a shows the reference force and two desired forces $\mathbf{F}_{d_2}$ and $\mathbf{F}_{d_3}$, both laying in (IV). Since the passivity constraint is not satisfied in joint 1, the only force that the device can create is a component of -$\mathbf{R}_{F_2}$ (i.e. $\tau_1 = 0, -\mathrm{R}_{F_1}$ = 0). For $\mathbf{F}_{d_2}$, the resulting force output is the projection of $\mathbf{F}_{d_2}$ onto -$\mathbf{R}_{F_2}$ i.e. $\mathbf{F}_{out_2}$, and for $\mathbf{F}_{d_3}$ the output force is $\mathbf{F}_{out_3}$. The output force has the same direction as -$\mathbf{R}_{F_2}$, with magnitude equal to the projection of the desired force on to the reference vector. Note, however, as the angle between the desired force and reference vector approaches 90°, the component of the displayable force tends to zero. Therefore, the output force generated by the n^{th} actuator in the partially displayable region is

$$\mathbf{F}_{out_n} = -\operatorname{sgn}(\dot{\theta}_n)\mathbf{R}_{F_n}\alpha_n \tag{5}$$

for $\dot{\theta}_n \neq 0$, and $0 \leq \alpha_n \leq 1$ where α_n is a controllable parameter modifying the magnitude of the output force, i.e.,

$$\alpha_n = \frac{\mathbf{F}_d \cdot \mathbf{R}_{F_n}}{||\mathbf{R}_{F_n}||^2}. \tag{6}$$

The boundary of the partly-displayable region is a vector orthogonal to the reference force direction. Since the reference velocities are columns of a Jacobian while the reference force vectors are rows of an inverse Jacobian, their product is an identity matrix:

$$\begin{bmatrix} 1 & 0 & 0 \\ 0 & \ddots & 0 \\ 0 & 0 & 1 \end{bmatrix} = \mathbf{J}^{-1}\,\mathbf{J} = \begin{bmatrix} \mathbf{R}_{F_1} \\ \vdots \\ \mathbf{R}_{F_i} \end{bmatrix} \begin{bmatrix} \mathbf{R}_{V_1} & \cdots & \mathbf{R}_{V_i} \end{bmatrix}. \tag{7}$$

Note that the multiplication of each term is equivalent to taking a dot product of the corresponding terms. If the dot product is 0 the vectors are orthogonal. Clearly, from the definition of the inverse matrix, each velocity vector is orthogonal to $i-1$ reference force vectors, and vice versa. Therefore, the limit of the partly-displayable region is defined by $\mathbf{R}_{F_i}$ and the $i-1$ orthogonal reference velocity vectors. For the manipulator in Fig. 1 the partially-displayable region (C) is bounded by +$\mathbf{R}_{V_1}$ and -$\mathbf{R}_{F_2}$, while region (D) is bounded by +$\mathbf{R}_{V_2}$ and -$\mathbf{R}_{F_1}$.

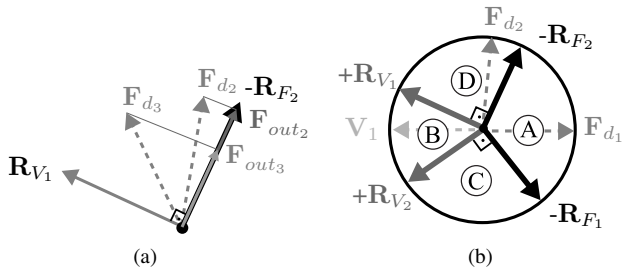

Fig. 3. (a) A projection of the desired forces along the force reference direction -$\mathbf{R}_{F_2}$. (b) For given velocity, $\mathbf{V}_1$, (I) ≋ (A) is fully displayable, (1) ≋ (B) is non-displayable, while (C) and (D) are partly-displayable.

3) Non-Displayable Region: The unaccounted range of forces that cannot be generated forms the *non-displayable region*, which is bounded by the velocity reference vector. For instance, the non-displayable region of $\mathbf{V}_1$ is (1) ≋ (B) as shown in Fig. 3b.

4) Uncontrollable Force Output: So far, we only considered a case where actuators are moving. Let us now consider the case where an actuator is stationary. In Fig. 4a, the input velocity $\mathbf{V}_2$ acts along +$\mathbf{R}_{V_1}$, making only the magnitude of -$\mathbf{R}_{F_1}$ controllable. The velocity along $\mathbf{R}_{V_2}$ (and $\dot{\theta}_2$), on the other hand, is zero. As a result, the force along $\mathbf{R}_{F_2}$ is no longer dependent on the velocity of the actator but per (2) it depends only on the force input.

In Fig. 4b, we observe the possible outputs of $\mathbf{R}_{F_2}$ resulting from $\mathbf{F}_{in_1}$ and $\mathbf{F}_{in_2}$. Since force $\mathbf{F}_{in_1}$ acts in line with the reference force direction, $\mathbf{F}_{out_1}$ is equal to -$\mathbf{R}_{F_2}$. On the other hand, $\mathbf{F}_{in_2}$ acts at an angle from the reference force, resulting in $\mathbf{F}_{out_2}$. The magnitude of the force output is equal to the projection of the force on the reference vector. Similar to the partial force displayed by a moving brake, the force output of a stationary actuator is

$$\mathbf{F}_{out_n} = -\frac{\mathbf{R}_{F_n}(\mathbf{F}_{in} \cdot \mathbf{R}_{F_n})}{||\mathbf{R}_{F_n}||^2}\beta_n \tag{8}$$

for $\dot{\theta}_n = 0$, and $\beta_n = \{0, 1\}$. Note that neither the magnitude nor the direction of the force output can be controlled. However, the brake may be turned off by setting $\beta_n = 0$. Whether the brake should be on or off is calculated with:

$$\beta_n = \operatorname{sgn}\left(\left[\mathbf{R}_{F_n}(-\mathbf{F}_{in} \cdot \mathbf{R}_{F_n})\right] \cdot \mathbf{F}_d\right) \tag{9}$$

This equation describes the force output of a static actuator and will be combined with (5) to form a general form of the output force equation in Section III.

III. Modelling a multi-DOF Device

The analysis developed in the previous section can be generalized to model a non-redundant device with n-DOF and determine the total force output. One can also determine all displayability regions found in any non-redundant passive device.

A. General Form of the Output Force

By combining (8) and (5) one can describe any force, in any of the displayability regions, for cases where actuators

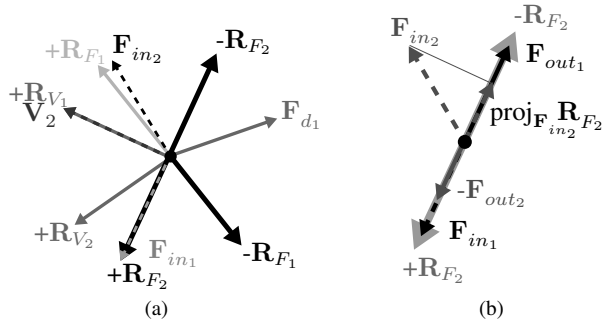

Fig. 4. (a) Depending on the force input, $\mathbf{F}_d$ can or cannot be produced. (b) Force output of a stationary actuator for different force inputs.

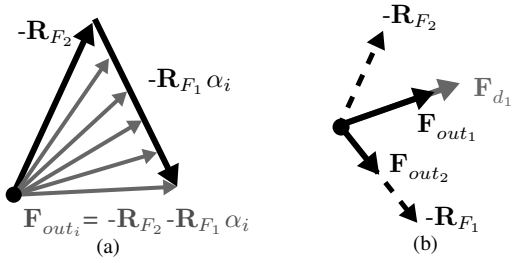

Fig. 5. (a) The force range generated using a controlled and an uncontrolled actuators. (b) The force generated due to $\mathbf{F}_{in_1}$ and $\mathbf{F}_{in_2}$

are moving or not, by summing the force output of each actuator i:

$$\mathbf{F}_{out} = \sum_{n=1}^{i} \begin{cases} -\operatorname{sgn}(\dot{\theta}_n)\mathbf{R}_{F_n}\alpha_n & \text{If } \dot{\theta}_n \neq 0, \\ & \text{and } 0 \leq \alpha_n \leq 1 \\ -\dfrac{\mathbf{R}_{F_n}(\mathbf{F}_{in}\cdot\mathbf{R}_{F_n})}{||\mathbf{R}_{F_n}||^2}\beta_n & \text{If } \dot{\theta}_n = 0, \\ & \text{and } \beta_n = \{0,1\} \\ 0 & \text{Otherwise.} \end{cases} \tag{10}$$

To display $\mathbf{F}_{d_1}$ in Fig. 4a, given $\mathbf{F}_{in_1}$ we must use the output of the stationary and moving actuator. In Fig. 5b we can see that the combined force output of the two actuators generates $\mathbf{F}_{out_1}$, which has the same direction as the $\mathbf{F}_{d_1}$. Note, however, that the magnitude of $\mathbf{F}_{out_1}$ is different from the magnitude of the desired force. As shown in Fig. 5a, the controllable force adds to the stationary actuator force and together they generate $\mathbf{F}_{out}$ = -$\mathbf{R}_{F_2}$-$\mathbf{R}_{F_1}\alpha_i$. Note, however, that we can only control either the magnitude or the direction of $\mathbf{F}_{out}$, but not both.

In contrast, when the same desired force is to be displayed with $\mathbf{F}_{in_2}$ acting on the device, the stationary brake must be off ($\beta_2 = 0$). The brake opposes the desired force, as shown in Fig. 5b, and the force output is the force of moving brake, i.e., $\mathbf{F}_{out_2}$=-$\mathbf{R}_{F_1}$ α. Further, (10) can be used to determine the number and type of regions in an n-DOF device.

B. Displayability Regions in an n-DOF Device

Let us examine the cases where all actuator are moving. The summation in (10) with a n-DOF device will involve n terms; one term for each actuator. The following three cases can be inferred:

- If the summation has no zero terms, the desired force is fully displayable.
- If at least one term of the summation is zero, the force is partially displayable
- If all terms are zero the forces are non-displayable.

Clearly, each combination of zero and non-zero terms corresponds to one displayability region. Considering all these 2^i combinations, we can find the number of regions in a device with i actuators. Moreover, the number of regions where k actuators can produce force is

$$\#\text{ of regions} = \frac{i!}{(i-k)!\,k!} \tag{11}$$

where $k = 0, 1, 2, \cdots, i$. The result for devices with-DOF between 1 and 6 is summarised in Table I.

Irrespective of the number of DOF, a passive haptic device always has 1 fully displayable ($k = i$) and 1 non-displayable region ($k = 0$); the remaining regions are partially displayable. These regions, however, differ from each other in the number of actuators they can use to partially display a force. Let us refer to this number as the *degree-of-displayability* (DOD), where DOD= k. In a 1-DOD region a force may be partially displayed using only one actuator, in a 2-DOD, two actuators, etc. So far, we have not seen regions with DOD greater than one. To understand the importance of these regions, let us examine a 3-DOF device which, according Table I, has two types of partially-displayable regions.

IV. Analyzing a 3-DOF Passive Device

Fig. 6a shows a 3-DOF non-redundant device with revolute joints. Its reference force and velocity vectors are found using (4) and are also shown in the figure. In this pose, all joints are orthogonal to one another. As a result, both force and velocity reference vectors will have the same direction. Note, however, if joints are not orthogonal these reference vectors will not be collinear, as was the case in Section II.

By using a single actuator, a force can be generated only along the reference direction. By controlling the magnitude of two reference vectors the resultant force vector forms an arc. Drawing the arcs for all combinations of the 3 reference forces forms a sphere with spherical triangles on the surface (see Fig. 6b). The surface area enclosed by these triangles represents the directions produced using all 3 reference vectors, similar to the regions found in a 2-DOF device.

For clarity, in Fig. 6b, let us shade in the surface of each triangle and project the resulting sphere onto top and bottom planes. In this representation, a direction vector appears as a point on the surface of the sphere (notice $\mathbf{V}_1$). Using this

TABLE I. Number of all regions in passive devices with various DOF.

DOF	Fully Disp.	Partly-Displayable with DOD = k					Non Disp.	Total Reg.
		$k=5$	$k=4$	$k=3$	$k=2$	$k=1$		
1	1	0	0	0	0	0	1	2
2	1	0	0	0	0	2	1	4
3	1	0	0	0	3	3	1	8
4	1	0	0	4	6	4	1	16
5	1	0	5	10	10	5	1	32
6	1	6	15	20	15	6	1	64

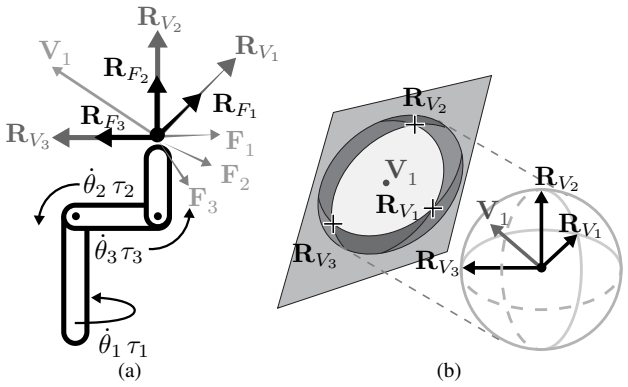

Fig. 6. (a) Reference vectors for a 3-DOF device, along with forces and velocities acting on the device. (b) A sphere representing all vector directions, and its projection onto a plane. The signs of the reference vectors are used to specify their position.

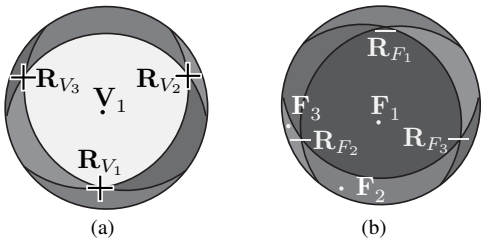

Fig. 7. Projections of the sphere: (a) top showing the non displayable region (b) bottom showing fully displayable region

representation, Fig. 7 shows the reference vectors, velocity, and forces acting on the manipulator in Fig. 6a.

As predicted by (11) and Table I, the device has a total of 8 regions: 1 displayable, 3 partly-displayable with 2 actuators (2-DOD), 3 partly-displayable with 1 actuator (1-DOD), and 1 non-displayable. These regions are the triangles on the projected spheres. The three displayable reference force vectors define the fully displayable region, while the non-displayable region is bounded by the reference velocity vectors. The remaining 6 regions are partially displayable.

The two types of partially displayable region can be seen in Fig. 7. Since arcs are formed by forces generated using 2 actuators, the regions sharing a side with the fully displayable region are partially displayable with the same two actuators. Consequently, the regions that share only a corner, that is a single reference vector, with the displayable region are partially displayable using only that one actuator. From this, we find that $\mathbf{F}_1$ is fully displayable, $\mathbf{F}_2$ can be partially displayed using a combination of -$\mathbf{R}_{F_2}$ and -$\mathbf{R}_{F_3}$, while $\mathbf{F}_3$ is partly-displayable using only -$\mathbf{R}_{F_2}$.

The displayable forces in regions with 1-DOD work in much the same way as the partly-displayable regions in a 2-DOF device described earlier. In these regions, the direction of the force is defined, and only the magnitude may be controlled. In the regions with 2-DOD, however, the direction of the force, along with its magnitude may be controlled using various combinations of the reference forces.

Lastly, moving from a 2-DOF to a 3-DOF device, there are significantly more directions that can be displayed using fewer than i actuators, i.e., there are 6 single actuator reference vectors, but there are also 12 regions where the force uses 2 actuators. Thus, a 3-DOF device may be more prone to stiction and to control the force output, the controller will rely more on the user's force input. From the control perspective, increasing the number of DOF has antagonistic effects on performance. On one hand, a larger portion of the workspace falls within partially displayable regions and the force approximation becomes more challenging.

V. Discussion

Based on the analysis of n-DOF devices in Section III we can compare devices with various DOF and gain insight into their feasibility. First, let us consider the relative size of the displayable region. This size varies widely depending on the configuration of the manipulator, therefore let us assume that all directions act orthogonal to one another, as was the case with the 3-DOF manipulator in Fig. 6a. In this configuration, all regions are equal in size. The number and type of each region can be found through (11). For any DOF, the number of fully-displayable and the non-displayable regions is 1. Thus, the relative size η of each of these two regions is

$$\eta = \frac{\text{\# of displayable regions}}{\text{\# of regions}} = \frac{1}{2^i} \tag{12}$$

Two observations can be made right away. For one, the relative size of the fully displayable region decreases exponentially as the number of DOF increases. Secondly, the size of the non-displayable region decreases at the same rate. As a result, forces can be displayed in an increasingly limited range of directions but there are also fewer forces that cannot be displayed at all.

To put it into perspective, the fully-displayable and the non-displayable regions account for 25% of all direction in a 2-DOF device. In 3-DOF manipulators, this number is only 12.5%, and at 6-DOF it drops to 1.6%. Since there is a small range of forces that can be displayed accurately, and an equally small range of forces that cannot be displayed at all, the majority of the force range is partially displayable.

Table I shows that as the number of DOF increases, so do the DOD of these regions. Increasing the DOD is crucial in improving the displayability of a passive device. Thus, in a 1-DOD region, like in partly-displayable regions found in a 2-DOF device, only the magnitude of the force output can be controlled. In contrast, both the magnitude and direction of the force in a 2-DOD region is controllable.

A well-designed controller should be able to make use of this additional freedom to improve the quality and/or accuracy of the forces produced by a passive device with many DOF. The controller could direct the user towards or away from regions with higher or lower DOD, respectively. Finally, with increasing DOF, the probability of one or more actuators in a device being stationary increases. As a result, a device with many DOF is likely to experience more stiction issues.

VI. Conclusions

Passively-actuated haptic devices are an alternative to the conventional haptic displays that employ electric motors.

Passive devices such as brakes have a high torque-to-volume ratio, low inertia, and they are intrinsically stable. On the other hand, the passivity of these devices makes them difficult to control. Several authors have highlighted issues with force control in passive devices. The majority of these analyses, however, have been limited to 2-DOF devices.

In this paper, we introduced a new framework to analyze the performance of an n-DOF haptic device using brakes as actuators. First, we reviewed the modelling techniques for a 2-DOF manipulator then expanded and generalized the analysis to examine the characteristics of an n-DOF device. The proposed formulation describes the quality of the force output generated in different regions of the workspace.

The analysis showed that as the number of DOF increases, the size of each region in the device decreases. In any non-redundant device, there is one fully and one non-displayable regions. As a result, the relative range of forces a device cannot produce decreases as the number of DOF increases. In fact, the range of forces in a haptic device with many DOF is mostly composed of partly-displayable regions.

An n-DOF device, additionally, contains many types of partly-displayable regions. These regions differ from each other in their degree-of-displayability (DOD), which represents the amount of control over a force produced in the partly-displayable regions. Higher DOD regions found in higher DOF devices offer better control over the force output. Using the partly-displayable forces and their full DOD, control algorithms may be able to greatly expand the range of a passive haptic device by approximating the desired force. In fact, using all the partly-displayable regions, the relative force range of an n-DOF device should approach the range of an equivalent active device.

Further, the analysis highlighted that a stationary actuator limits the control over the force output of a device. The number of directions where one or more actuators is stationary increases with the number of DOF. As a result, a passive device with a high number of DOF will be more prone to stiction problems. However, [20]–[22] showed that the stiction may be, in part, mitigated by using clever control schemes. As a result, the feasibility of a device with n-DOF also depends on the controller's ability to alleviate problems caused by stiction and approximate a desired force.

Using partly-displayable forces produces an error in the reproduction of the force. For purposes of simulation, however, these forces do not have to be perfectly accurate. Humans have well-studied perception thresholds. For instance, according to [25], the sensory threshold of a human user is 7% for a differential change in force magnitude and, according to [26], 5° for change in direction. If the controller can maintain these differential errors within this range, a device with n-DOF will be feasible in many applications.

REFERENCES

[1] J. E. Colgate and G. G. Schenkel, "Passivity of a class of sampled-data systems: Application to haptic interfaces," *J. of robotic syst.*, vol. 14, no. 1, pp. 37–47, 1997.

[2] V. Hayward and K. E. MacLean, "Do it yourself haptics: part I," *IEEE Robotics & Automation Maga.*, vol. 14, no. 4, 2007.

[3] J. An and D.-S. Kwon, "Five-bar linkage haptic device with DC motors and MR brakes," *J. of Intelligent Material Syst. and Structures*, vol. 20, no. 1, pp. 97–107, 2009.

[4] A. D. McCarthy *et al.*, "Passive haptics in a knee arthroscopy simulator: is it valid for core skills training?" *Clinical Orthopaedics and Related Research (1976-2007)*, vol. 442, pp. 13–20, 2006.

[5] C. Rossa, J. Lozada, and A. Micaelli, "A new hybrid actuator approach for force-feedback devices," in *IEEE/RSJ Int. Conf. on Intelligent Robots and Syst. (IROS)*. IEEE, 2012, pp. 4054–4059.

[6] ——, "Design and control of a dual unidirectional brake hybrid actuation system for haptic devices," *IEEE Trans. on Haptics*, vol. 7, no. 4, pp. 442–453, 2014.

[7] C. Rossa *et al.*, "Design considerations for magnetorheological brakes," *IEEE/ASME Trans. on Mechatronics*, vol. 19, no. 5, pp. 1669–1680, 2013.

[8] N. Najmaei *et al.*, "Design and performance evaluation of a prototype MRF-based haptic interface for medical applications," *IEEE/ASME Trans. on Mechatronics*, vol. 21, no. 1, pp. 110–121, 2016.

[9] D. Senkal, H. Gurocak, and E. I. Konukseven, "Passive haptic interface with MR-brakes for dental implant surgery," *Presence: Teleoperators and Virtual Environments*, vol. 20, no. 3, pp. 207–222, 2011.

[10] J. Troccaz and Y. Delnondedieu, "Semi-active guiding systems in surgery. a two-DOF prototype of the passive arm with dynamic constraints (PADyC)," *Mechatronics*, vol. 6, no. 4, pp. 399–421, 1996.

[11] N. Najmaei, M. R. Kermani, and R. V. Patel, "Suitability of small-scale magnetorheological fluid-based clutches in haptic interfaces for improved performance," *IEEE/ASME Trans. on Mechatronics*, vol. 20, no. 4, pp. 1863–1874, 2015.

[12] J.-S. Oh, S.-H. Choi, and S.-B. Choi, "Control of repulsive force in a virtual environment using an electrorheological haptic master for a surgical robot application," *Smart Materials and Structures*, vol. 23, no. 1, p. 015010, 2013.

[13] M. Sakaguchi, J. Furusho, and N. Takesue, "Passive force display using ER brakes and its control experiments," in *IEEE Pro. Virtual Reality*. IEEE, 2001, pp. 7–12.

[14] A. Khanicheh *et al.*, "MR compatible ERF driven hand rehabilitation device," in *9th Int. Conf. on Rehabilitation Robotics (ICORR)*. IEEE, 2005, pp. 7–12.

[15] J. Nikitczuk, B. Weinberg, and C. Mavroidis, "Control of electrorheological fluid-based torque generation components for use in active rehabilitation devices," in *Smart Materials and Structures*, vol. 6174. SPIE, 2006, p. 61742C.

[16] W. J. Book *et al.*, "The concept and implementation of a passive trajectory enhancing robot." Georgia Institute of Technology, 1996.

[17] M. R. Reed and W. J. Book, "Modeling and control of an improved dissipative passive haptic display," in *IEEE Int. Conf. on Robotics and Automation (ICRA)*, vol. 1. IEEE, 2004, pp. 311–318.

[18] C. Cho, M. Kim, and J.-B. Song, "Performance analysis of a 2-link haptic device with electric brakes," in *Symp. on Haptic Interfaces for Virtual Environment and Teleoperator Syst.* IEEE, 2003, pp. 47–53.

[19] C. Cho, J.-B. Song, and M. Kim, "Design and control of a planar haptic device with passive actuators based on passive force manipulability ellipsoid (FME) analysis," *J. of Robotic Syst.*, vol. 22, no. 9, pp. 475–486, 2005.

[20] C. Cho, M. Kim, and J.-B. Song, "Direct control of a passive haptic device based on passive force manipulability ellipsoid analysis," *Int. J. of Control, Automation, and Syst.*, vol. 2, no. 2, pp. 238–246, 2004.

[21] D. K. Swanson and W. J. Book, "Obstacle avoidance methods for a passive haptic display," in *IEEE/ASME Int. Conf. on Advanced Intelligent Mechatronics*, vol. 2. IEEE, 2001, pp. 1187–1192.

[22] C. Cho, J.-B. Song, and M. Kim, "Energy-based control of a haptic device using brakes," *IEEE Trans. Syst. Cybern.*, vol. 37, no. 2, pp. 341–349, 2007.

[23] D. Karnopp, "Computer simulation of stick-slip friction in mechanical dynamic systems," *J. of dynamic syst. measurement, and control*, vol. 107, no. 1, pp. 100–103, 1985.

[24] J. Duffy, *Statics and Kinematics with Applications to Robotics*. Cambridge University Press, 1996.

[25] X.-D. Pang, H. Z. Tan, and N. I. Durlach, "Manual discrimination of force using active finger motion," *Perception & psychophysics*, vol. 49, no. 6, pp. 531–540, 1991.

[26] J. Voisin, Y. Lamarre, and C. E. Chapman, "Haptic discrimination of object shape in humans: contribution of cutaneous and proprioceptive inputs," *Experimental Brain Res.*, vol. 145, no. 2, pp. 251–260, 2002.